

## Coercivity of a percolative magnetic system

José Mejía-López,<sup>1,2</sup> Ricardo Ramírez,<sup>1</sup> Miguel Kiwi,<sup>1</sup> Michael J. Pechan,<sup>3</sup> J. Zachary Hilt,<sup>3</sup> S. Kim,<sup>4</sup> Harry Suhl,<sup>4</sup> and Ivan K. Schuller<sup>4</sup>

<sup>1</sup>Facultad de Física, Pontificia Universidad Católica, Casilla 306, Santiago, Chile 6904411

<sup>2</sup>Facultad de Ciencias, Escuela Superior Politécnica de Chimborazo, Panamericana Sur, Km 1, Riobamba, Ecuador

<sup>3</sup>Department of Physics, Miami University, Oxford, Ohio 45056

<sup>4</sup>Physics Department, University of California-San Diego, La Jolla, California 92093-0319

(Received 9 June 2000; published 27 December 2000)

A model that describes the behavior of the coercivity  $H_c$ , of coalescing Ni films, as a percolation phenomenon is presented. We show that there is a nonmonotonic dependence, of the coercive field as a function of the occupation probability  $p$ . This behavior is a function of cluster size and topology, and is independent of the growth direction of the thin film. Based on these ideas we predict theoretically, and confirm experimentally, the dependence of  $H_c$  as a function of external magnetic field orientation. For a [111] oriented fcc film, if  $p$  is less than the percolation threshold  $p_{cr}$ , a sixfold symmetry is observed. However, if  $p \approx p_{cr}$  the percolation is isotropic.

DOI: 10.1103/PhysRevB.63.060401

PACS number(s): 75.70.Cn, 75.70.Kw, 64.60.Ak

The concept of percolation was introduced in the realm of science by Broadbent and Hammersley<sup>1</sup> in 1957. Since then, it has been applied to many problems in completely different fields, ranging from natural sciences to sociological phenomena.<sup>2</sup> In physics, percolation has been useful in the study of microscopic<sup>3</sup> as well as macroscopic phenomena.<sup>4,5</sup> In particular, granular systems inherently prone to percolation, have experimentally shown magnetic anomalies when the grains are magnetic. Panina *et al.*<sup>6</sup> found that the effective magnetic permeability of composite materials containing small Fe particles (of 1–2  $\mu\text{m}$  size) tends to zero near the percolation threshold. Xiao and Chien<sup>7</sup> observed that across the whole volume fraction range, in granular Fe-(SiO<sub>2</sub>) solids, magnetic coercivity experiences dramatic variations due to the change of grain size and percolation effects. In thin films the relation between magnetism and percolation also has been investigated: for example, the transition from superparamagnetism to ferromagnetism,<sup>8</sup> while recently Gor'kov and Kresin<sup>9</sup> studied the transition from paramagnetic to conducting ferromagnetic phases of manganites by percolation theory. Moreover, Choi *et al.*<sup>10</sup> observed that the coercivity  $H_c$  of Ni films, whose magnetic and structural properties are found in the literature,<sup>11</sup> exhibits a nonmonotonic behavior, related to topological morphology changes, which coincides with the onset of percolation. However, no theoretical ideas have been advanced which directly connect coercivity and percolation.

In order to study changes in  $H_c$  as a function of morphology in Ni, Choi *et al.*<sup>10</sup> performed a well controlled experiment evaporating Ni films, by molecular beam epitaxy (MBE), on top of various thickness  $t_{\text{Cu}}$  copper buffer layers. The morphology of the Cu buffer layer changes with  $t_{\text{Cu}}$ . First isolated copper clusters form, but as  $t_{\text{Cu}}$  increases pairs of clusters coalesce. As more Cu is deposited a critical thickness is reached and the Ni covered Cu clusters percolate. In order to assure that all changes in the coercivity of Ni are due only to changes in morphology, all other structural parameters of the epitaxial Ni were kept constant. These parameters include: the thickness (100 Å), the level of contamination,

the growth parameters, the capping layer width (150 Å of Al), the (111) crystalline orientation perpendicular to the substrate, and the mosaic spread. All these structural and chemical properties were checked using *in situ* Auger electron spectroscopy (AES), reflection high energy electron diffraction (RHEED), low energy electron diffraction (LEED) and *ex situ* x-ray diffraction (XRD), scanning electron microscopy (SEM), and atomic force microscopy (AFM).

Two major variations of the coercivity  $H_c$  become apparent as the morphology reaches the percolation threshold; the magnitude of  $H_c$  changes in a nonmonotonic fashion and the in-plane angular anisotropy changes as well. Both of them display a distinct feature, which coincides with the crossing of the percolation threshold. Our theoretical model explains these two distinct features, that is: (i) the magnitude of  $H_c$  as a function of the copper substrate thickness; and (ii) the dependence of  $H_c$  on the direction of the applied field  $H$ . The model shows that  $H_c$ , as a function of site occupation probability  $p$ , has a nonmonotonic dependence due to the fractional variation of the cluster sizes and their topology, as they form during the film deposition process, and it is also shown that this behavior is independent of the growth direction of the magnetic film. Moreover, also the symmetry of  $H_c$ , when  $p \approx p_{cr}$ , is in quantitative agreement with experiment.

Our model focuses upon the morphological changes that take place during the growth of a thin film, which in its early stage is characterized by a homogeneous distribution of the small islands. When additional material is deposited these islands grow in size, due to the large mobility of the small droplets, until coalescence sufficient for percolation is achieved. Based on this the coercivity  $H_c(p)$ , as a function of occupation probability  $p$ , can be understood assuming that the magnetization reversal mechanism depends on cluster size and topology: (i) if the particles are smaller than a certain critical size  $z_{cr}$ , of the order of a domain wall,  $H_c$  is large, due to the fact that for such particles wall nucleation is energetically unfavorable. Consequently, the magnetization

reversal proceeds, for instance, through coherent rotation of the spins;<sup>12</sup> (ii) for simply connected particles, whose sizes are greater than  $z_{cr}$ , the coercive field  $H_c$  is smaller than the former since now a domain wall<sup>13</sup> can nucleate. Thus, the magnetization reversal is achieved by processes that require less energy, predominantly by domain wall nucleation and displacement; and (iii) larger clusters may be multiply connected and the domain walls might get pinned by the voids, especially if these are of considerable size. Thus, when the fraction of voids is large enough the inversion mechanism depends both on cluster size and topology, since domain wall formation is likely, but their propagation is hindered by pinning to the voids that are present.

As usual  $H_c$  is defined as the reversal field required to achieve zero magnetization. To determine the coercivity we introduce the reduced magnetization  $M_\mu(H)$ , which corresponds to the quotient between the actual and the saturation magnetization of a single cluster. The indices  $\mu = s, b$ , and  $v$  label clusters of the type (i), (ii), and (iii), as described above. Thus, the analytic expression for the film magnetization  $M(H)$  is

$$M(H) = \rho_s M_s(H) + \rho_v M_v(H) + (1 - \rho_s - \rho_v) M_b(H), \quad (1)$$

where  $\rho_\mu$  is the fractional area occupied by each type of clusters. Consequently we obtain the coercivity  $H_c$  solving the equation  $M(H_c) = 0$ .

The fractional areas  $\rho_s$  and  $\rho_v$ , of the different type clusters, are obtained by using the Monte Carlo technique.<sup>14</sup> In this algorithm each of the  $L$  sites of a lattice is occupied by a particle with probability  $p$ . This produces a configuration of  $Lp$  particles. A cluster is defined as follows: two occupied sites belong to same cluster if they are nearest neighbors. The calculation is iterated keeping all the parameters (system size and occupation probability) fixed and changing the configuration of the particles adopt. The final values of  $\rho_s$  and  $\rho_v$  are obtained averaging over a number of random configurations. Convergence is obtained after  $10^3$  Monte Carlo steps and averaging over ten random configuration.

We now formulate a criterion to classify a cluster as belonging to type (iii) as defined above. Designating as  $f$  the ratio between the number of empty sites inside a cluster  $\eta_e$  and the number of occupied sites in the same cluster  $\eta_o$ , that is  $f = \eta_e / \eta_o$ , we classify the cluster as belonging to class (iii) if  $f > f_{cr}$ .

Moreover, we make the following simple assumption: that only two types of islands are important, as far as magnetic properties are concerned. Clusters of type (i) and (iii), with broader loops, switch by magnetization rotation, while the larger type (ii) ones, with narrower loops, only switch after they nucleate a domain wall. To obtain  $H_c$  as a function of  $p$  we need to know the form of  $M_s(H) = M_v(H)$  and  $M_b(H)$  in the region  $H = 0$  to  $H_b$ , and we denote as  $H_b$  and  $H_s$  the broad and narrow loop values, respectively. The approximations we use to fit the experimental relations between magnetization and applied field  $M_\mu(H)$  are

$$M_\mu(H) = M_r \tanh\left(\frac{H + H_\mu}{2q_\mu}\right), \quad (2)$$

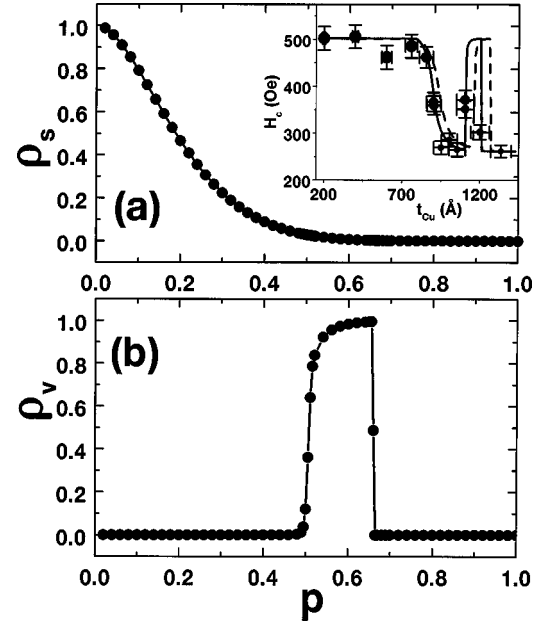


FIG. 1. (a) Small cluster fractional area as a function of  $p$ , which is related to the Cu thickness through Eq. (3). (b) Fractional area of large clusters with voids as a function of  $p$ . The insert is the coercivity  $H_c$  (Oe) as a function of Cu thickness  $t_{Cu}$  ( $\text{\AA}$ ) observed experimentally at 5 K. The continuous (dashed) line is obtained using our model for a  $1000 \times 1000$  triangular (square) lattice. The parameters used are  $M_r = 0.69$ ,  $q_s = q_b = 50$  (Oe),  $z_{cr} = 2$ , and  $f_{cr} = 0.5$ . The circles are experimental data from Choi *et al.*

where  $M_r$  is the reduced remanent magnetization,  $\mu = s$  and  $b$ , and  $q_\mu^{-1}$  is proportional to the slope of the corresponding hysteresis loop at  $M_\mu = 0$ .

The results of implementing the model outlined above are given in Fig. 1. As expected, the fractional area of small clusters  $\rho_s \approx 1$  for  $p \ll 1$ , and decreases to  $\rho_s \approx 0$  as  $p$  grows. On the other hand, the fractional area  $\rho_v \approx 0$  for  $p \ll 1$  and grows very fast when the percolation threshold is approached. Finally,  $\rho_v$  undergoes an abrupt drop when the dominant contribution is due to the formation of large clusters without voids. The kinks of  $\rho_v$  arise from finite-size effects. Replacing the numerical data obtained for  $\rho_s$  and  $\rho_v$ , and combining Eq. (2) with  $M(H_c) = 0$ , we obtain the coercivity as a function of  $p$  as displayed in the insert of Fig. 1(a).

In order to make further progress an assumption has to be made on the unknown relation between the experimentally measured<sup>10</sup> copper layer thickness  $t_{Cu}$  and  $p$ . We choose the simplest alternative: a linear relation. The two values required to determine this fit are chosen as follows: (i) the minimum of  $H_c$ ; and (ii) the value for which  $H_c$  versus  $p$ , in the insert of Fig. 1, ceases to be flat as a function of  $t_{Cu}$ . This yields

$$t_{Cu} [\text{\AA}] = 780p + 650. \quad (3)$$

The above fit is certainly not unique, but depends on the value we adopt for  $z_{cr}$ . Consequently, this fit is valid only for  $650 \leq t_{Cu} [\text{\AA}] \leq 1430$ . However, the results for  $H_c$  we obtain for  $650 \leq t_{Cu} [\text{\AA}]$  are insensitive to this choice and

thus we refrain from postulating a more sophisticated fit, which would imply additional parameters.

On the basis of the experiments we adopt  $M_r=0.69$  for both switching mechanisms, since it was observed that  $M_r$  does not depend  $t_{Cu}$ . For the slopes we adopt  $q_s=q_b=50$  (Oe), and stress the fact that the main features of  $H_c=H_c(p)$  do not depend on the detailed form of  $M_s(H)$  and  $M_b(H)$ . In fact, we found no significant changes in the behavior of  $H_c$  for two extreme cases: (a) a rectangular hysteresis loop, and (b) assuming linear fits of  $M_s(H)$  [ $M_b(H)$ ] which go through  $H_s$  [ $H_b$ ] and  $M_r$ . Always (i) if  $p \ll p_{cr}$  then  $H_c$  versus  $p$  is flat, since a single switching mechanism dominates and thus  $H_c=H_s$ ; (ii) independent of the form of  $M_s(H)$  and  $M_b(H)$  a minimum is obtained around the percolation threshold  $p_{cr}$ ; and, (iii) a maximum of  $H_c$  appears for  $p > p_{cr}$ , which decays to the minimum value of  $H_c$  as  $p$  grows. This behavior is insensitive to the form of  $M_s(H)$  and  $M_b(H)$ . We employed the value  $f_{cr}=0.5$  in the insert Fig. 1(a); changing the latter only narrows or enhances the width of the  $p > p_{cr}$  maximum. The fact that the  $H_c$  versus  $t_{Cu}$ , displayed in the insert, is similar both for triangular and square lattices is a strong indication that this behavior is universal, i.e., does not depend on the growth direction of the thin film.

On the other hand, the angular dependence of the coercivity is also modified by percolation. For the small clusters we consider a single domain thin film, with its surface oriented in the [111] direction. In spherical coordinates the direction of the magnetization  $\vec{M}$  is defined by the angles  $\theta$  and  $\phi$  that  $\vec{M}$  makes with the Cartesian axes ( $z$  axis is oriented along the [111] direction, while the  $x$  axis is parallel to the  $[\bar{1}10]$  direction). The film parameters are defined as follows:  $K$  is an effective anisotropy constant and  $M_0$  is the saturation magnetization. The external field  $H$  is confined to the  $x,y$  plane, and  $\phi_H$  is the angle between  $H$  and  $x$ .

Three terms contribute to the total energy (per unit volume)  $E_T$ : the magnetocrystalline anisotropy  $E_K$ , the Zeeman term  $E_Z$  and the magnetostatic energy  $E_M$ .  $E_K$  determines the easy magnetization directions, which lie along the diagonals of the cubic cell (in the [111],  $[\bar{1}11]$ ,  $[1\bar{1}1]$ , and  $[\bar{1}\bar{1}\bar{1}]$  directions). In this coordinate system

$$E_K = -\frac{\sqrt{2}}{3} K \sin^3 \theta \cos \theta \sin(3\phi) + \frac{K}{12} \cos^2 \theta (6 - 7 \cos^2 \theta), \quad (4)$$

$$E_Z = -HM_0 \sin \theta \cos(\phi - \theta_H), \quad (5)$$

$$E_M = -2\pi N M_0^2 \sin^2 \theta, \quad (6)$$

where  $N$  is the demagnetizing factor. Defining the dimensionless energy  $\varepsilon = 3E_T/K$ , we can write

$$\varepsilon = \varepsilon_1 - h \sin \theta \cos(\phi - \theta_H), \quad (7)$$

where  $\varepsilon_1 = 3(E_K + E_M)/K$  and  $h = 3M_0 H/K$ . For equilibrium it is required that  $\partial\varepsilon/\partial\theta=0$  and  $\partial\varepsilon/\partial\phi=0$ . Stable (unstable) equilibrium is attained if the determinant of the associated Hessian matrix is positive (negative). As the

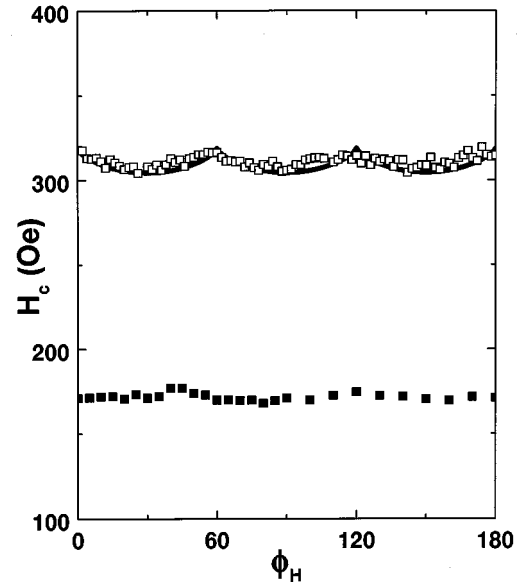


FIG. 2. Coercivity  $H_c$  as a function of the magnetic field direction  $\phi_H$ . The continuous line is the theoretical sixfold fit of the experimental data depicted, for  $p \leq p_{cr}$ , by the full dots. The full squares illustrate the isotropic dependence of  $H_c$  versus  $\phi_H$  for  $p \approx p_{cr}$ , which corresponds to  $t_{Cu}=100$  nm, measured at room temperature. The experimental error is smaller than the size of the full dots and squares.

(negative) field intensity  $H$  is increased,  $M$  rotates first gradually and then abruptly towards the unstable field direction. Analytically this is fulfilled when one of the following conditions is satisfied:  $\partial^2\varepsilon/\partial\theta^2=0$  or  $\partial^2\varepsilon/\partial\phi^2=0$ .

The dimensionless field  $h$  can thus be evaluated. However, only the lowest negative eigenvalue obtained for  $h$  is physically meaningful; we make sure that this corresponds to a crossover from a minimum to a maximum by checking the sign of  $\partial^3\varepsilon/\partial\theta^3$ . Figure 2 compares the results of these calculations with experiment; the error bars of the latter are smaller than the size of the dots in the figure. The parameters used in the computations are:  $M_0=500$  G,<sup>15</sup>  $K=2022$  erg/cm<sup>3</sup>,<sup>16</sup> and the demagnetization factor  $N=0.05$ . Assuming a Gaussian distribution of the anisotropy axes of magnetic clusters around the mean orientation, it is found analytically that  $K$  is reduced<sup>16</sup> in good agreement with the fits obtained from Fig. 2.

$H_c$  has a sixfold symmetry, related to the fact that we are dealing with the (111) face. However, an additional condition is also required: that the spins adopt a small out of the (111) plane component, since otherwise the sixfold symmetry is quenched. Thus, as the system is rotated around the [111] axis [perpendicular to the (111) plane] the spins are barely drawn towards the easy [111] axis, all in satisfactory agreement with experiment.<sup>17</sup>

On the other hand, when the percolation threshold  $p_{cr}$  is reached, the system behavior is dominated by the large clusters. In that case, the dipolar interaction becomes larger and has the effect of aligning in plane the total magnetization of the cluster. Thus the anisotropy energy  $E_K(\theta=\pi/2)=0$  is independent of  $\phi$ , which was verified experimentally<sup>17</sup> as shown in Fig. 2. A very small orientation dependence of the

coercive field is observed beyond the percolation limit which may be understood as follows: reversal in that limit takes place by domain-wall nucleation followed by wall motion. Nucleation may be sensitive to orientation, but since it takes place in only a small fraction of a cluster, and since the rate of wall motion is presumably much less sensitive to orientation, the overall anisotropic effect is very small.

In conclusion, we have developed a model which displays and provides an understanding for the relation between coercivity  $H_c$  and percolation. This relation is a consequence of morphological changes in the magnetic system and was recently observed experimentally.<sup>10</sup> We showed that the observed behavior is due to a geometric property of two-dimensional lattices, in particular, to the relative number of clusters larger and smaller than a critical size. Small size clusters switch their magnetization, under an external field, through simple spin rotation. The larger clusters reverse their magnetization, by nucleation and motion of domain walls.

Below the percolation threshold  $p_{cr}$  most of the clusters are small, and thus the  $H_c$  versus  $t_{Cu}$  relation in Fig. 1 is flat. The decrease of  $H_c$  is related to the increase in the number of

large clusters, until they exceed the number of small ones, allowing a crossover from magnetization rotation to domain-wall nucleation and motion, to be the dominant magnetization switching mechanism. However, there is an increase of  $H_c$ , in the vicinity of  $p_{cr}$ , since inside the clusters the presence of internal nearest neighbors empty sites pin the domain-wall displacement. Finally,  $H_c$  decreases up to its continuous film value, since as  $p$  grows a single large cluster forms. We have also shown that, when a fcc film is grown in the [111] orientation, a sixfold symmetry of  $H_c$  for  $p < p_{cr}$  exists, which crosses over to an isotropic behavior for  $p \approx p_{cr}$ .

M.K. and J.M.L. gratefully acknowledge Dr. Ruben D. Portugal and Professor Marcos Kiwi for stimulating discussions. This work was partially supported by the US-DOE at Miami, AFOSR-MURI at UCSD and FONDECYT, Chile under Grant Nos. 2980013 and 8990005. H.S. acknowledges partial support by the Center for Magnetic Recording Research at UCSD.

- 
- <sup>1</sup>R. Broadbent and J. M. Hammersley, Proc. Cambridge Philos. Soc. **53**, 629 (1957).  
<sup>2</sup>J. W. Essam, Rep. Prog. Phys. **45**, 574 (1973); D. Stauffer, *Introduction to Percolation Theory* (Taylor & Francis, London, 1994).  
<sup>3</sup>P. W. Anderson, in *Ill-Condensed Matter*, edited by R. Balion, R. Marynard, and G. Toulouse (North-Holland, Amsterdam, 1979).  
<sup>4</sup>M. Hori and F. Yonezawa, J. Phys. C **10**, 229 (1977).  
<sup>5</sup>W. T. Elam *et al.*, Phys. Rev. Lett. **54**, 701 (1985).  
<sup>6</sup>L. V. Panina *et al.*, J. Appl. Phys. **76**, 6365 (1994).  
<sup>7</sup>G. Xiao and C. L. Chien, Appl. Phys. Lett. **51**, 1280 (1987).  
<sup>8</sup>H. J. Elmers *et al.*, Phys. Rev. Lett. **73**, 898 (1994).  
<sup>9</sup>L. P. Gor'kov and V. Z. Kresin, Pis'ma Zh. Eksp. Teor. Fiz. **67**, 934 (1998) [JETP Lett. **67**, 985 (1998)].  
<sup>10</sup>J. M. Choi *et al.*, J. Magn. Magn. Mater. **191**, 54 (1999).  
<sup>11</sup>G. Bochi *et al.*, Phys. Rev. B **52**, 7311 (1995).  
<sup>12</sup>E. Stoner and E. P. Wohlfarth, Philos. Trans. R. Soc. London, Ser. A **240**, 74 (1948); E. H. Frei, S. Shtrikman, and D. Treves, Phys. Rev. **106**, 446 (1957).  
<sup>13</sup>H. Suhl and H. N. Bertram, J. Appl. Phys. **82**, 6128 (1997).  
<sup>14</sup>K. Binder and D. W. Heermann, *Monte Carlo Simulation in Statistical Physics* (Springer-Verlag, Berlin, 1992).  
<sup>15</sup>A. P. Guimarães and I. S. Oliveira, *Magnetism and Magnetic Resonance in Solids* (John Wiley & Sons, New York, 1998).  
<sup>16</sup> $E_\kappa = \frac{1}{2} \kappa \cos[6(\theta - \theta_0)]$ , where  $\kappa$  is the bulk anisotropy constant. If the axis direction  $\theta_0$  is assumed to have a Gaussian distribution of width  $\Delta$ , then  $\langle E_\kappa \rangle = \frac{1}{2} \kappa \exp(-9\Delta^2) \cos(6\theta)$ . For  $\Delta \approx 25^\circ$  this yields  $K \approx \kappa/10$ .  
<sup>17</sup>Experimentally, the  $\phi_H$  dependence of the coercive field  $H_c$  was obtained at room temperature on a vibrating sample magnetometer. The values were obtained from full  $M-H$  loops that were taken at  $2^\circ$  intervals, for in-plane angles from zero through  $180^\circ$  or  $360^\circ$ , depending upon the sample. All samples exhibited sixfold symmetry below  $p_{cr}$ , similar to that displayed in Fig. 2.